

06,07,13

Effect of the heterovalent cation substitution $\text{Bi}^{3+} \rightarrow \text{Ba}^{2+}$ in BaTiO_3 on the phase transition $Pm-3m \leftrightarrow P4mm$ and efficiency of energy harvesting

© V.D. Fokina¹, M.V. Gorev^{1,2}, V.S. Bondarev^{1,2}, M.S. Molokeev^{1,2}, I.N. Flerov¹

¹Kirensky Institute of Physics, Federal Research Center KSC SB RAS, Krasnoyarsk, Russia

²Institute of Engineering Physics and Radioelectronics, Siberian Federal University, Krasnoyarsk, Russia

E-mail: fokina@iph.krasn.ru

Received August 14, 2024

Revised August 24, 2024

Accepted August 25, 2024

The heat capacity, thermal expansion and sensitivity to change of electric field of ceramic samples BaTiO_3 and $\text{Ba}_{0.97}\text{Bi}_{0.02}\text{TiO}_3$ were studied. The nature of the influence of chemical pressure and electric field on the main parameters of the phase transition $Pm-3m \leftrightarrow P4mm$ was revealed. The Olsen thermodynamic cycle was analyzed in the entropy-temperature diagram and the densities of the converted waste heat energy into electrical energy were determined.

Keywords: phase transitions, ferroelectrics, heat capacity, thermal expansion, energy harvesting.

DOI: 10.61011/PSS.2024.10.59632.214

1. Introduction

The ever-growing demand for electricity is primarily covered (by about 76%) by the use of non-renewable energy sources, while heat remains the main source [1]. Heat losses remain quite significant despite significant progress in optimization of traditional cycles with heat supply from fuel combustion (oil, gas, coal). Devices employing a direct thermodynamic cycle can be considered as renewable or, at least, sustainable energy sources in case of successful harvesting of the wasted energy since the temperature level of wasted energy is very often quite high. The problem of energy harvesting and storage is very relevant nowadays in view of the above circumstances.

An actively developed approach using the pyroelectric effect stands out among numerous methods of utilization of („waste“) energy based on a variety of physical effects [2–6]. Pyroelectric generators are solid-state heat engines that convert thermal energy directly into electrical energy, since any change of temperature in pyroelectric energy harvesting devices results in an electrical potential difference at the terminals of the generator.

Ferroelectrics and antiferroelectrics, as well as relaxors, are considered as promising materials (bulk ceramics, thick/thin films) for use as working bodies in thermodynamic energy conversion cycles based on the pyroelectric effect. Most of the studied ferroelectric ceramics until recently have been produced on the basis of $\text{Pb}(\text{Zr}_x\text{Ti}_{1-x})\text{O}_3$ and $\text{Pb}(\text{Mg}_{1/3}\text{Nb}_{2/3})\text{O}_3$ or their solid solutions [7–12]. High content (about 60%) of highly toxic lead is the main disadvantage of such materials, which does not conform with modern environmental requirements for micro- and

nanoelectronics functional elements [13–16]. Lead-free ferroelectric materials [13–16] have been the subject of numerous active studies in recent years for this particular reason. At the same time, the primary attention is paid to solid solutions based on BaTiO_3 , $\text{Bi}_{0.5}\text{Na}_{0.5}\text{TiO}_3$ and $\text{K}_{0.5}\text{Na}_{0.5}\text{NbO}_3$.

It was found that partial substitution of cations in different crystallographic positions of BaTiO_3 structure can result not only in a change of the temperature of ferroelectric structural transformation and wedging of intermediate phases, but also in the occurrence of relaxor properties. So, for example, the region of existence of an anomalous heat capacity associated with the phase transition $Pm-3m \leftrightarrow P4mm$ significantly expands (almost 100 K) and the behavior of the corresponding dielectric constant deviates from the classical Curie–Weiss law when Sn^{4+} and Zr^{4+} ions isovalent to titanium are introduced in BaTiO_3 , which indicates the smearing of the ferroelectric transformation and, thus, the evolution of materials closer to the relaxor state [17–20].

The generally recognized optimal thermodynamic cycle for collecting the waste heat energy is the cycle proposed by R.B. Olsen and consisting of two isothermal and two isofield processes [21,22]. As a rule, the Olsen cycle is analyzed in P – E coordinates in case of implementation of processes in the following sequence: $T_{\text{cold}}=\text{const}$ ($E_{\text{low}} \rightarrow E_{\text{high}} \rightarrow E_{\text{high}}=\text{const}$ ($T_{\text{cold}} \rightarrow T_{\text{hot}} \rightarrow T_{\text{hot}}=\text{const}$ ($E_{\text{high}} \rightarrow E_{\text{low}} \rightarrow E_{\text{low}}=\text{const}$ ($T_{\text{hot}} \rightarrow T_{\text{cold}}$). The specific electrical work performed within the cycle, also known as energy density (J/cm^3), determined by integrating the cycle area, is used for quantifying the degree of efficiency of using a specific ferroelectric as a working body: $N_D = \oint E dP$.

Recently, when studying a solid solution of $\text{BaTi}_{0.86}\text{Sn}_{0.14}\text{O}_3$ (BTSn) synthesized by homovalent substitution of the central atom, we tested for the first time the possibility of using a comparative analysis of the Olsen cycle within the framework of two phase diagrams: polarization–electric field and entropy–temperature [19]. A satisfactory agreement was found between the energy density values determined using two approaches, which confirmed the possibility of using data on the heat capacity measured under conditions of $E = 0$ and $E \neq 0$ for evaluation of the efficiency of usage of a specific material as a working fluid in the energy harvesting cycle.

This paper studies the effect of heterovalent substitution of divalent barium with trivalent bismuth in the interoctahedral cavity of the structure of $Pm\text{-}3m$ on heat capacity, thermal expansion, its sensitivity to changes of the electric field and characteristics of the energy harvesting efficiency of compounds of $\text{Ba}_{1-x}\text{Bi}_{2x/3}\text{TiO}_3$ ($x = 0, 0.03$). Previously, such solid solutions were studied for determining the degree of sensitivity of phase transition temperatures and dielectric properties to changes of chemical pressure [23].

2. Samples and experimental methods

Compounds of BaTiO_3 (BT) and $\text{Ba}_{0.97}\text{Bi}_{0.02}\text{TiO}_3$ (BBT) were obtained as a result of a solid-phase reaction of $(1-x)\text{BaCO}_3 + x/3\text{Bi}_2\text{O}_3 + \text{TiO}_2 \rightarrow \text{Ba}_{1-x}\text{Bi}_{2x/3}\text{TiO}_3 + (1-x)\text{CO}_2$ according to the procedure described in Ref. [24]. The input materials were thoroughly ground for one hour, and then compressed into discs under a pressure of 100 MPa. Synthesis was carried out at 1100°C for 2 h. The samples were annealed at 850°C for 15 h at the last stage. As a result, ceramic cylindrical tablets ($d = 7$ mm, $h = 1.1$ mm) were obtained with the density of $\sim 92\%$ of the theoretical one. Gold electrodes were applied to ceramic samples by sputtering in a vacuum for studying the dielectric constant and the effect of the electric field on the parameters of the phase transition.

The structural characterization of the synthesized BT and BBT samples was performed at 300 K using Haoyuan DX-2700BH powder X-ray diffractometer with Cu-K α radiation and a linear detector. The size of step 2θ was 0.01°, the exposure at each point was 0.2 s per step. All peaks in the experimental diffractograms were indexed in a tetragonal cell ($P4mm$) with parameters close to those of BaTiO_3 . Therefore, this structure was adopted as a starting model for refinement by the Rietveld method, which was performed using TOPAS 4.2 software [25]. The refinements were stable and gave low R -factors (Figure 1, Table 1). No impurities or foreign phases were found in both samples. The position of the Ba^{2+} ion in the BBT structure was occupied by $\text{Ba}^{2+}/\text{Bi}^{3+}$ ions with a fixed ratio according to the proposed chemical formula, $\text{Ba}_{0.97}\text{Bi}_{0.02}\text{TiO}_3$.

Detailed measurements of the isobaric heat capacity $C_p(T)$ in the temperature range 310–415 K were performed using an automatic adiabatic calorimeter [26]. The

Table 1. Main parameters of the study of the structure of ceramic samples of $\text{Ba}_{1-x}\text{Bi}_{2x/3}\text{TiO}_3$ ($x = 0; 0.03$) at 300 K

Compound	BaTiO_3	$\text{Ba}_{0.97}\text{Bi}_{0.02}\text{TiO}_3$
Space group	$P4mm$	$P4mm$
a (Å)	3.99117(40)	3.99612(17)
c (Å)	4.03015(49)	4.02771(17)
V (Å ³)	64.198(15)	64.318(6)
Z	1	1
2θ -interval, °	15–70	15–70
R_{wp} , %	11.015	6.45
R_p , %	7.694	4.53
χ^2	4.279	3.61
R_B , %	8.96	0.98

samples were placed in a measuring cell with a heater and secured with Apiezon grease, which ensured a reliable thermal contact. The heat capacity of the samples was measured in continuous ($dT/dt = 0.2\text{--}0.4$ K/min) and discrete ($\Delta T = 1.5\text{--}3.0$ K) heating modes with an error not exceeding 0.3–1.0%. The heat capacity of a measuring cell with a heater was measured in a separate experiment.

The temperature dependences of linear deformation $\Delta L/L(T)$ and the coefficient of linear thermal expansion $\alpha(T)$ were studied using Netzsch induction dilatometer DIL-402C in a flow of gaseous helium with a flow rate of 50 ml/min. The sample heating rate was 2/min. The experiments were performed in the absence of ($E_{cp} = 0$) and the application ($E = 5.45$ kV/cm) of an electric field. A fused silica standard was used to calibrate and account for the expansion of the measurement system. The consistency of the data obtained in several series of measurements was quite high $\sim 97\%$.

The dielectric permittivity of $\text{Ba}_{1-x}\text{Bi}_{2x/3}\text{TiO}_3$ ceramics was measured using device E7-20 at a frequency of 1 kHz. The experiments were carried out in a dilatometer in parallel with measurements of thermal expansion on the same samples.

3. Results and discussion

The results of the study of the temperature behavior of the heat capacity of $\text{Ba}_{1-x}\text{Bi}_{2x/3}\text{TiO}_3$ ceramics are shown in Figure 2. An anomalous behavior of $C_p(T)$ was detected which was associated with the transition during heating from the tetragonal phase $P4mm$ to the initial cubic phase $Pm\text{-}3m$.

It can be seen that the cationic substitution of $\text{Bi}^{3+} \rightarrow \text{Ba}^{2+}$ resulted in the smearing of the peak heat

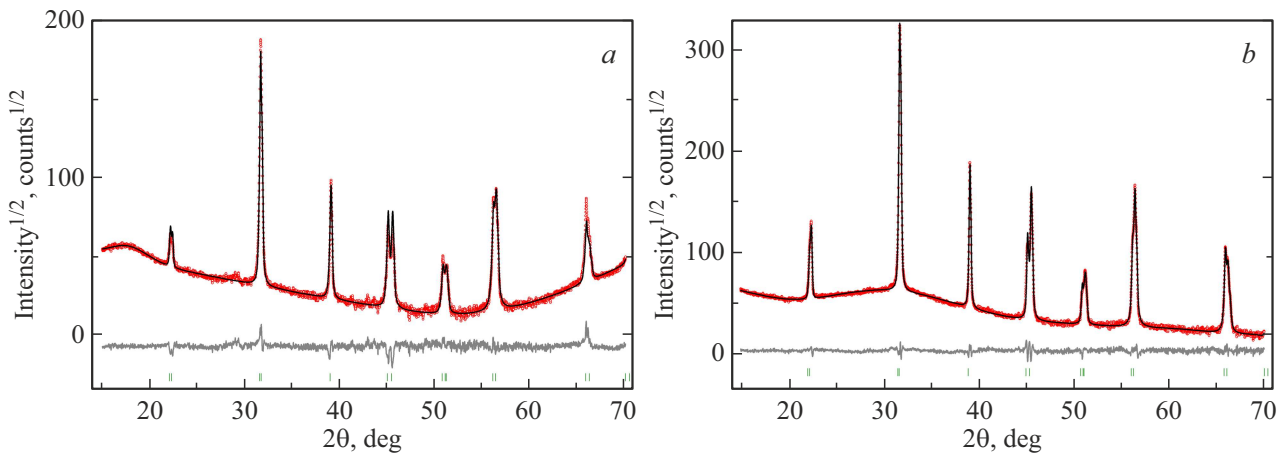


Figure 1. Difference X-ray diffraction pattern of the study of the structure in the phase of $P4mm$ BT (a) and BBT (b) at 300 K.

capacity of BBT and in a significant decrease of its maximum value compared to BT. At the same time, the temperatures of the maxima C_p , T_1 , interpreted as structural transformation temperatures, turned out to be quite close to 397 K (BT) and 402 K (BBT).

To determine the integral thermodynamic characteristic, namely, the change of entropy due to a change of the symmetry of the crystal lattice, resulting in the occurrence of polarization, it was necessary to divide the total molar heat capacity into components corresponding to the lattice $C_{\text{Lat}}(T)$ and anomalous contributions associated with polarization $\Delta C_p(T) \sim \partial P^2/\partial T$. The sections on the curve $C_p(T)$ outside the area of the heat capacity anomaly were considered as corresponding to $C_{\text{Lat}}(T)$ and approximated by a combination of Debye and Einstein functions $C_{\text{Lat}}(T) = K_D C_D(T, \theta_D) + K_E C_E(T, \Theta_E)$, where K_D , K_E , θ_D , Θ_E are fitting parameters.

The integration of temperature dependences $\Delta C_p/T$ made it possible to determine the entropy changes in

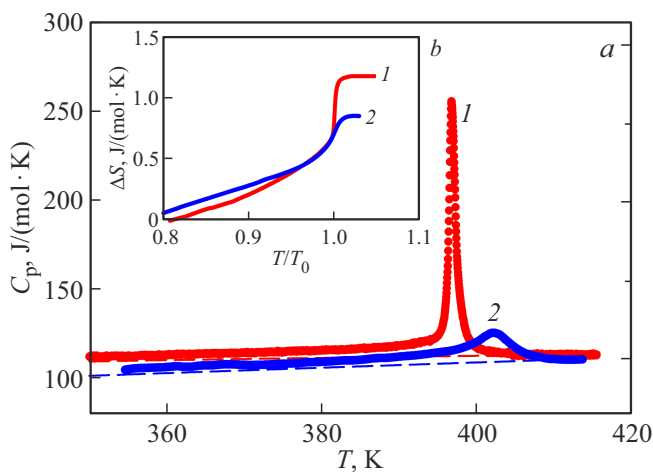


Figure 2. Temperature dependences of isobaric molar heat capacity (a) and anomalous entropy (b) of ceramics BT (1) and BBT (2). Dashed lines — lattice heat capacities.

case of the phase transition $Pm-3m \leftrightarrow P4mm$ for both studied ceramic samples: $\Delta S_1 = (1.3 \pm 0.1) \text{ J/mol} \cdot \text{K}$ (BT) and $\Delta S_1 = (0.9 \pm 0.1) \text{ J/mol} \cdot \text{K}$ (BBT). It follows from the temperature dependences $\Delta S_1(T)$ shown in Figure 2 that a change of chemical pressure due to partial cationic substitution resulted not only in a decrease of the entropy of the transition to BBT, but also in a change of the nature of its behavior: there is no significant increase C_p in the vicinity of T_1 , related to latent heat. These results suggest that a slight change of chemical pressure changed the type of phase transition $Pm-3m \leftrightarrow P4mm$ from the first to the second.

Figure 3, a shows the results of measurements of BT and BBT thermal expansion. The transition to the tetragonal phase in both compounds is accompanied by a pronounced abnormal behavior of the linear thermal expansion coefficient $\alpha(T)$. At the same time, the peak value $\alpha(T)$ in BBT turned out to be smaller and more smoothed. Phase transition temperatures: 400 K (BT) and 404 K (BBT), corresponding to the minima $\alpha(T)$, although slightly, but still higher than similar temperatures determined by calorimetric measurements. The discrepancy between the values of T_1 determined by two thermophysical methods is explained by different experimental conditions, namely, different rates of temperature change. The conditions for the process of measurement of heat capacity $dT/dt \leq 0.4 \text{ K/min}$ are closer to equilibrium thermodynamic conditions in comparison with the process of measuring thermal expansion, $dT/dt = 2 \text{ K/min}$.

The nature of the impact of the electric field on the ferroelectric transformation temperature $Pm-3m \leftrightarrow P4mm$ and the behavior of a number of physical properties of BT was known [27,28]. Therefore, we experimentally determined the stability of the cubic phase to changes in the electric field, that is, the dependence $T_1(E)$, only for BBT. Thermal expansion experiments on a single sample were performed under the conditions of $E = 0$ and $E \neq 0$. The results of the study turned out to be reproducible in several series of repeated measurements and are provided

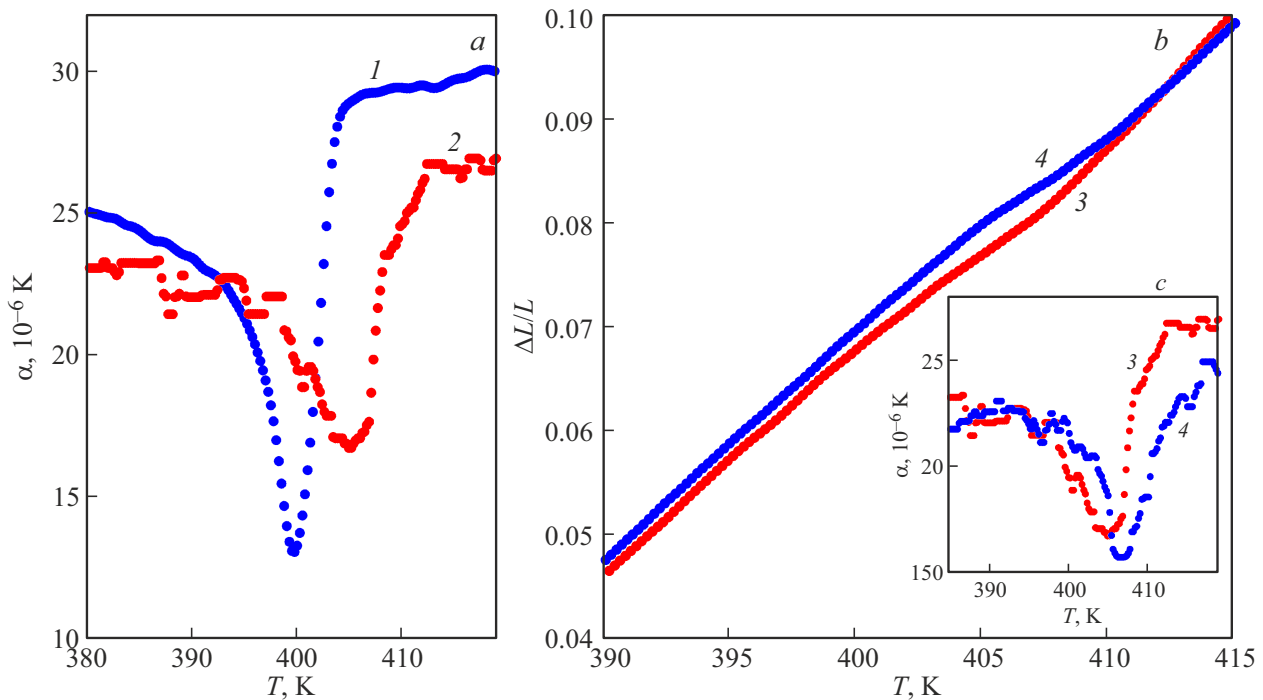


Figure 3. Temperature behavior of the coefficient of linear thermal expansion of BT (1) and BBT (2) ceramics in the vicinity of the phase transition $Pm\text{-}3m \leftrightarrow P4mm$ (a). Temperature dependences of deformation $\Delta L/L$ (b) and α (c) for BBT ceramics at $E = 0$ (3) and $E = 5.45$ kV/cm (4).

in Figures 3, b and 3, c. The phase transition temperature shift at $E \neq 0$ is most clearly manifested in the dependence $\alpha(T, E)$ (Figure 3, c). It turned out that the field with the intensity of $E = 5.45$ kV/cm increases the temperature of phase transition $Pm\text{-}3m \rightarrow P4mm$ corresponding to the minimum of the peak $\alpha(T)$, by ~ 2 K. It was not possible to perform measurements in fields of higher intensity due to the design of the dilatometer measuring chamber. It was difficult to obtaining reliable data at lower values of E due to the small magnitude of the change T_1 . Therefore, the coefficient characterizing the sensitivity of the BBT solid solution to the electric field was determined from two experimental points and amounted to $dT_1/dE = 0.37$ K/(kV/cm). There is no reason to doubt the reliability of the coefficient value in connection with the above-mentioned high reproducibility of the measurement results of thermal expansion during thermal cycling. Moreover, the value of dT_1/dE turned out to be somewhat smaller, but still close to the values previously established for single-crystal BaTiO_3 in experiments studying the effect of an electric field on birefringence, $dT_1/dE = 0.75$ K/(kV/cm) [28], and the heat capacity, $dT_1/dE = 0.55$ K/(kV/cm) [27]. The difference in the values obtained by different methods is quite likely attributable, firstly, to different intervals of the electric field: $\Delta n_{[100]}(T, -E) - (0-1.5-3.2)$ kV/cm and $C_p(T, E) - (0-3.5-5.9)$ kV/cm, and secondly, to different experimental boundary conditions: $(\Delta n_{[100]})_{T=\text{const}}(E)$ and $(C_p)_{E=\text{const}}(T)$.

The value of the rate of change of the transition temperature under the action of an electric field for BT was also determined by us from the Clapeyron–Clausius equation: $dT_1/dE = \delta P/\delta S$. However, calculations were performed using more precisely determined quantities of ΔP [29] and ΔS since for this ferroelectric the jumps of polarization δP and entropy δS at T_1 are close to their complete changes [26]. The calculated coefficient, $dT_1/dE = 0.77$ K/(kV/cm), agrees well with the values determined experimentally.

Therefore, the nature of the effect of changes in chemical pressure and electric field strength on the phase transition $Pm\text{-}3m \leftrightarrow P4mm$ in BT is identical in a number of positions. Firstly, the temperature T_1 increases in both cases. It cannot be excluded that this may be attributable to an increase of the volume of the lattice cell, since the hydrostatic pressure causing a decrease of the volume of the BT lattice cell results in a decrease of the temperature T_1 [30].

Secondly, it was previously discovered in Ref. [27] that the transition of the first kind $Pm\text{-}3m \leftrightarrow P4mm$ in BT approaches the tricritical point with an increase of the electric field strength, and a similar phenomenon in the BBT solid solution is evidenced by the smoothing of the heat capacity anomaly compared to with BT.

The temperature dependences of the dielectric constant BT and BBT are shown in Figure 4, a and 4, b. In the vicinity of room temperature, the permittivity values of both compounds are close, on the order of $\sim 10^3$. However, the presence of trivalent Bi in the perovskite structure

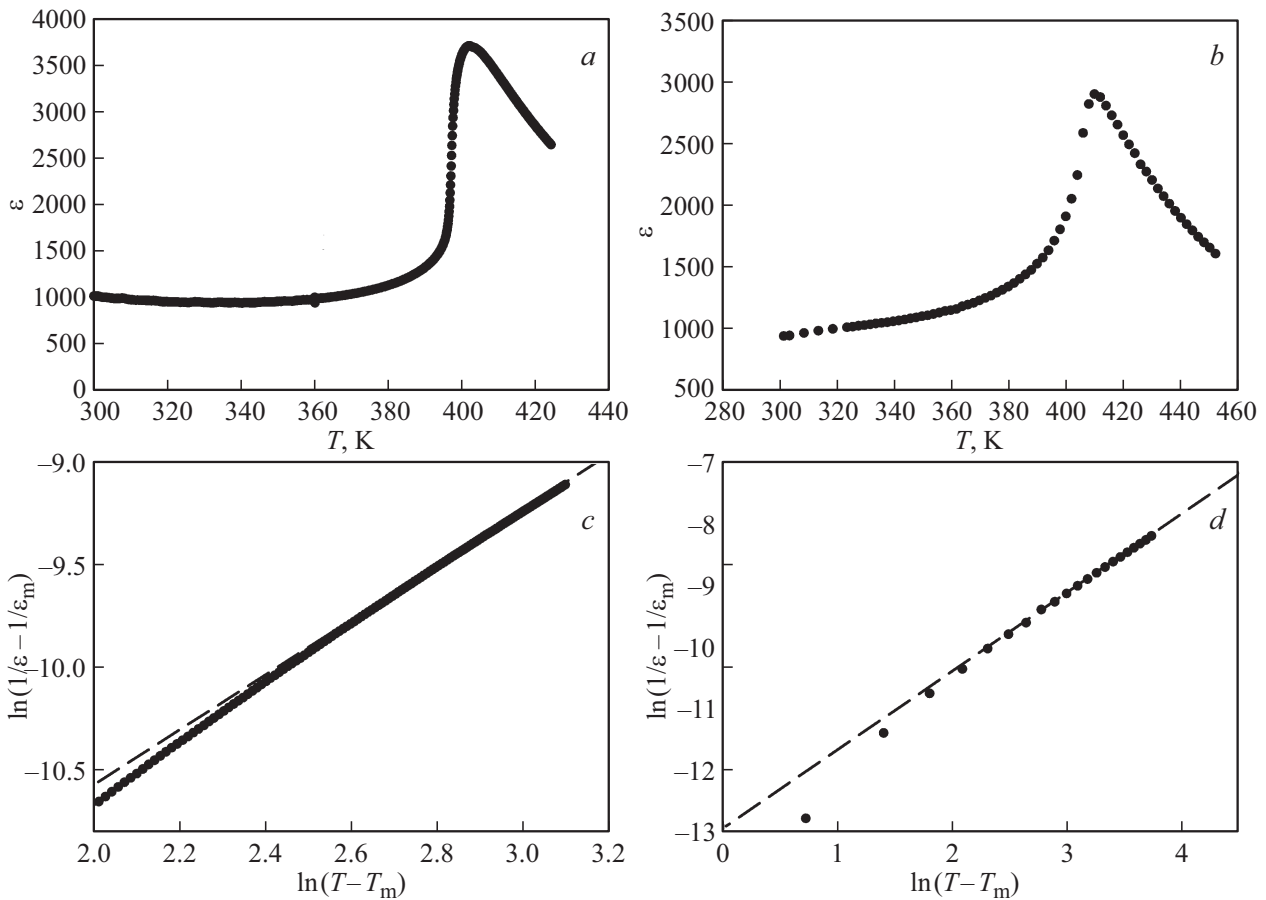


Figure 4. Temperature dependences of the dielectric constant BT (a) and BBT (b) at $f = 1$ kHz. The behavior of the value $\ln(1/\varepsilon - 1/\varepsilon_m)$ as a function of $\ln(T - T_m)$ for BT (c) and BBT (d).

resulted in the expansion of the peak $\varepsilon(T)$ during the phase transition $Pm-3m \rightarrow P4mm$ and a decrease of its maximum value from 3700 for barium titanate to 2900 in solid solution.

The dependencies $\varepsilon(T)$ were described using a universal equation known as modified Curie–Weiss law and obtained based on the analysis of both a composition fluctuation microscopic model [31,32] and empirical data for smeared phase transitions [33], $(1/\varepsilon - 1/\varepsilon_m) = (T - T_m)^\gamma / C''$, where ε_m — the maximum value of the dielectric constant at corresponding temperature T_m , C'' — modified Curie–Weiss constant and the parameter γ is 1 for classical ferroelectrics and 2 for relaxors. The intermediate values γ characterize the degree of diffusivity (smearing) of the phase transition.

Figure 4, c and d show the dependence of the logarithm of the inverse permittivity. The values of γ for „pure“ barium titanate and solid solution were 1.34 and 1.27, respectively, which indicates a fairly small degree of smearing of the ferroelectric transition. The value of $\gamma > 1$ is related to the ceramic nature of the studied sample. The occurrence of internal mechanical stresses is inevitable, leading to some smearing of anomalies of physical properties due to the dimensional heterogeneity and random orientation of

crystalline grains in ceramics. The results obtained are consistent with the data that BBT solid solutions in the bismuth concentration range $0 < x < 0.09$ undergo ferroelectric transitions $Pm-3m \leftrightarrow P4mm$, and the transitions have a relaxor nature at $0.09 < x < 0.15$ [34].

It was impossible to obtain reliable information about the dielectric hysteresis loops due to the sufficiently high electrical conductivity of the BT and BBT ceramic samples. However, as we have recently shown, the isofield dependences of entropy in the diagram $S-T$ can be used for determining the parameters of energy harvesting along with the isotherms in the diagram $P-E$: the energy density values N_D , calculated by two methods were satisfactorily consistent between themselves [19].

Since direct measurements of the heat capacity under the conditions of $E \neq 0$ were impossible due to the release of Joule heat due to the high conductivity of ceramics, the following procedure was performed to restore the function of $S(T, E \neq 0)$. First, it was assumed that the entropy of the phase transition $Pm-3m \leftrightarrow P4mm$, ΔS_1 , does not depend on the electric field, at least with its low intensity $E_{high} = 5.45$ kV/cm used in the paper. Secondly, the position of the anomalous entropy on the lattice component at $E_{high} \neq 0$, $\Delta S_1(T, E)$, was determined

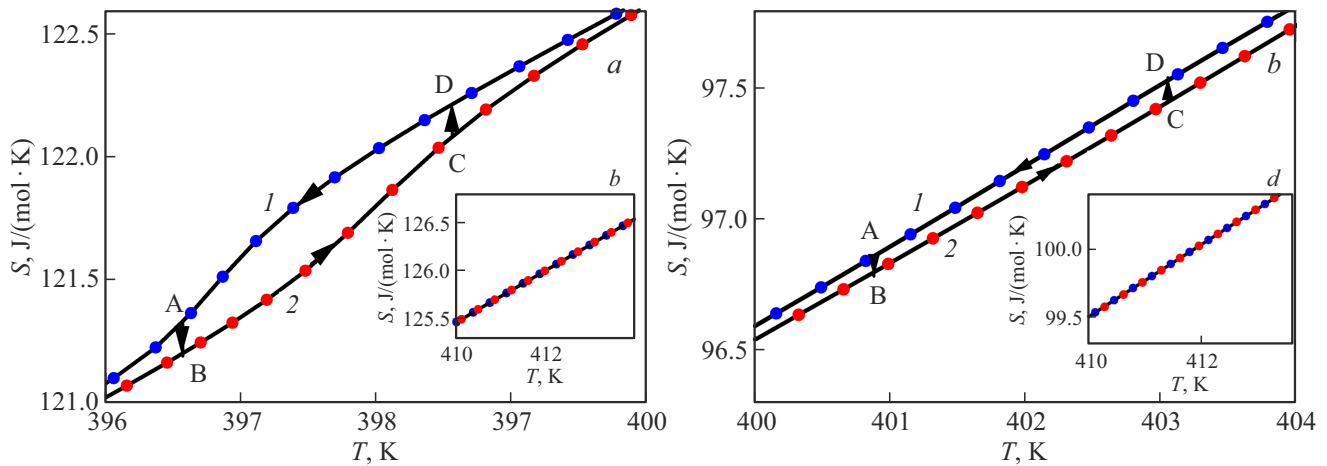


Figure 5. Temperature dependences of the molar entropy of BT (*a, b*) and BBT (*c, d*) ceramics at $E_{\text{low}} = 0$ (*1*) and $E_{\text{high}} = 5.45 \text{ kV/cm}$ (*2*) in the vicinity of the phase transition $Pm\bar{3}m \leftrightarrow P4mm$ (*a, c*) and in the paraelectric phase (*b, d*).

Table 2. Comparison of absolute N_D and relative N_D^* energy densities for various bulk and thick-film (BTSn) ferroelectric materials. (& — data from these studies)

Material	$N_D, \text{ J/cm}^3$	$T_{\text{cold}}, \text{ K}$	$T_{\text{hot}}, \text{ K}$	$E_{\text{low}}, \text{ kV/cm}$	$E_{\text{high}}, \text{ kV/cm}$	$N_D^* \cdot 10^5, \text{ J/(cm}^2 \cdot \text{kV} \cdot \text{K)}$	References
PMN-10PT	0.19	303	353	0	35	10.9	[35]
8/65/35PLZT	0.89	298	433	2	75	9.0	[36]
BCT-BZT-Fe	0.30	303	483	0	30	5.5	[37]
BTSn (P-E)	0.127	220	320	0	18.5	6.8	[19]
BTSn (S-T)	0.168	220	320	0	15.4	10.9	[19]
BT (S-T)	0.032	310	410	0	5.5	5.9	&
BBT (S-T)	0.043	310	410	0	5.5	7.8	&

by shifting the function $\Delta S_1(T, E = 0)$ along the temperature scale in accordance with the coefficient dT_1/dE : $\Delta S_1(T, E_{\text{high}}) = \Delta S_1(T + E_{\text{high}} \cdot dT_1/dE, 0)$.

Figure 5 shows the temperature dependences of the total entropy $S(T) = \int (CP/T)_E dT$ of both studied ceramics in the phase transition region at T_1 corresponding to the conditions $E_{\text{low}} = 0$ and $E_{\text{high}} = 5.45 \text{ kV/cm}$. In accordance with the data shown in Figure 2, *b*, the impact of the electric field is more clearly manifested for BT, and *c* with coefficients dT_1/dE one and a half times different. At the same time, the curves $S(T, E_{\text{low}} = 0)$ and $S(T, E_{\text{high}} \neq 0)$ coincide in the paraelectric phase, i.e., where there is no polarization and the associated abnormal entropy (Figure 5, *b* and *d*).

The energy harvesting cycles of A-B-C-D-A in coordinates S – T are shown in Figure 5, *a* and *c*. The A-B process is isothermal, associated with an increase of the external field strength from $E_{\text{low}} = 0$ to $E_{\text{high}} = 5.45 \text{ kV/cm}$. Further, the working body is heated from T_{cold} to T_{hot} at $E_{\text{high}} = \text{const}$ in the process of B-C by supplying „waste“ heat from an external source. The electric field decreases to zero in the isothermal process C-D. And finally, the ceramic working

body returns under conditions of $E_{\text{low}} = 0$ to the original temperature T_{cold} in the D-A process. The area of the cycle constructed in this way will be equal to the energy density collected in one cycle.

A-B-C-D-A cycles are presented in a narrow temperature range in Figure 5, *a* and *c*. The temperature range, at least, 70–100 K is of practical interest from the point of view of recycling „of waste“ low-potential heat. Therefore, we estimated the density of the collected energy, $N_D = \oint T dS$, for both samples during the cycle in the temperature range from $T_{\text{cold}} = 310 \text{ K}$ to $T_{\text{hot}} = 410 \text{ K}$ and presented the estimates in Table 2, where information about the energy harvesting parameters of related ferroelectric materials based on PbTiO_3 and BaTiO_3 is also provided for comparison. It can be seen that the ferroelectrics BT and BBT studied by us are significantly inferior in terms of energy density N_D to all the materials shown in Table 2.

On the other hand, Table 2 shows that it is very difficult to compare the results of various studies conducted on related compounds because of very different ranges of both temperatures $T_{\text{hot}} - T_{\text{cold}}$ and electric fields $E_{\text{high}} - E_{\text{low}}$ used

to determine energy harvesting parameters. It can be assumed that there are at least two main reasons for this situation. First, the temperature range is strongly related to the temperature of the „normal“, T_1 , or diffuse, T_m , phase transition. Secondly, the maximum value of the field used E_{high} is certainly limited by the breakdown voltage, which is individual for each of the samples and is rarely given in articles.

Therefore, a comparison of relative values of the following type, $N_D^* = N_D / (\Delta T \cdot \Delta E)$, in our opinion, is more correct and informative based on the results provided in Ref. [19]. Of course, the dependencies $N_D(T)$ and $N_D(E)$ for fixed intervals $E_{high} - E_{low}$ and $T_{hot} - T_{cold}$ should be close to linear in this case. However, these conditions are not exotic, since similar dependences were observed in wide ranges of external parameters for both BTSn solid solution [19] and BCT-BZT-Fe ceramics [37].

Table 2 shows that both studied samples, BT and BBT, like other lead-free perovskites, are practically not inferior to lead-containing compounds in terms of the relative efficiency parameter N_D^* . It is safe to assume that the correspondence of the energy densities obtained for different materials will be even more satisfactory at equally high values of E_{high} , E_{low} and T_{hot} , T_{cold} . As for the studied BT and BBT ceramics, the obvious task for the future is to improve the technology of their production, which would make it possible to significantly reduce the conductivity of the samples.

4. Conclusion

Temperature dependences of heat capacity, thermal expansion and dielectric constant of ceramic samples of $Ba_{1-x}Bi_{2x/3}TiO_3$ ($x = 0; 0.03$) were studied in the region of ferroelectric phase transition $Pm-3m \leftrightarrow P4mm$. A small percentage substitution of the Ba^{2+} cation by Bi^{3+} in the $BaTiO_3$ structure led to the following consequences, a number of which are consistent with the effects observed under pressure and/or in electric field conditions.

First, the volume of the lattice cell slightly increased in the phase $P4mm$ of BT solid solution despite the ratio of ionic radii, $R_{Bi^{3+}} < R_{Ba^{2+}}$ (CN=12) (Table. 1), which, apparently, can be explained by a nontrivial change in interatomic interactions due to heterovalent cation substitution.

Secondly, an increase of the temperature of the phase transition in BBT was found, which is probably caused by the said increase of the volume of the lattice cell, since the external hydrostatic pressure causing a decrease of the volume results in a decrease of temperature T_1 [30].

Thirdly, cationic substitution did not change the behavior of the dielectric constant, as evidenced by the persistency of the indicator $\gamma \approx 1.3$ in the modified Curie–Weiss equation.

Fourth, the sensitivity of the transition temperature to a change in the electric field has decreased, as evidenced by

a one and a half to two times decrease in the coefficient dT_1/dE for BBT compared to BT.

Fifth, the behavior of the heat capacity implies a change of the first kind of phase transition in BT to the second kind in BBT, which is consistent with the approximation of this transformation to the tricritical point at $E \neq 0$ in BT [24].

Sixth, the analysis of the isofield temperature dependences of the total entropy indicates a slight difference in the relative densities of the utilized energy in the Olsen cycles with BT and BBT as working bodies and their proximity to the parameters of other promising ferroelectric materials (Table 2).

Acknowledgments

X-ray and dilatometric data were obtained using the equipment of the Krasnoyarsk Regional Center for Collective Use of the Federal Research Center Krasnoyarsk Scientific Center of the Siberian Branch of the Russian Academy of Sciences.

Funding

The study was carried out within the framework of the research topic of the State Assignment of the Institute of Physics of the Siberian Branch of the Russian Academy of Sciences.

Conflict of interest

The authors declare that they have no conflict of interest.

References

- [1] IRENA. REthinking Energy 2017 (2017).
- [2] G. Sebald, D. Guyomar, A. Agbossou. *Smart Mater. Struct.* **18**, 125006 (2009).
- [3] S. Pandya1, J. Wilbur, J. Kim, R. Gao, A. Dasgupta, C. Dames, L.W. Martin. *Nature Mater.* **17**, 432 (2018)
- [4] A. Thakre, A. Kumar, H.-C. Song, D.-Y. Jeong, J. Ryu. *Sensors* **19**, 2170 (2019).
- [5] R.A. Surmenev, R.V. Chernozem, I.O. Pariy, M.A. Surmeneva. *Nano Energy* **79**, 105442 (2021).
- [6] D. Zabek, F. Morini. *Therm. Sci. Eng. Prog.* **9**, 235 (2019).
- [7] G.H. Haertling. *J. Am. Soc.* **82**, 797 (1999).
- [8] N. Setter, R. Wasser. *Acta Mater.* **48**, 151 (2000).
- [9] G. Rijnders, D.H. Blank. *Nature* **433**, 369 (2005).
- [10] S. Choi, T.R. Shrout, S. Jang, A. Bhalla. *Mater. Lett.* **8**, 253 (1989).
- [11] X.-G. Tang, H.L.-W. Chan. *J. Appl. Phys.* **90**, 034109 (2005).
- [12] R. Yimnirun, A. Ngamjarujana, R. Wongmaneeung, S. Wongsanmai, S. Ananta, Y. Laosiritaworn. *Appl. Phys. A* **89**, 737 (2007).
- [13] A. Chauhan, S. Patel, G. Vats, R. Vaish. *Energy Technol.* **2**, 205 (2014).
- [14] A. Chauhan, S. Patel, R. Vaish. *AIP Adv.* **4**, 087106 (2014).
- [15] S. Patel, A. Chauhan, R. Vaish. *Energy Technol.* **3**, 70 (2015).
- [16] S. Patel, A. Chauhan, A. Chauhan, R. Vaish. *Mater. Res. Express* **2**, 035501 (2015).

- [17] M.V. Gorev, V.S. Bondarev, I.N. Flerov, F. Sue, J.-M. Savario. *FTT* **47**, 12, 2212 (2005). (in Russian).
- [18] A.A. Instan, K.K. Mishra, R.S. Katiyar. *J. Appl. Phys.* **126**, 134101 (2019).
- [19] V.D. Fokina, V.S. Bondarev, E.I. Pogoreltsev, I.N. Flerov. *Ceramics International* **48**, 32966 (2022).
- [20] C. Lei, A.A. Bokov, Z.-G. Ye. *J. Appl. Phys.* **101**, 084105 (2007).
- [21] R.B. Olsen, D.D. Brown. *Ferroelectrics* **40**, 17 (1982).
- [22] R.B. Olsen, D.A. Bruno, J.M. Briscoe. *J. Appl. Phys.* **58**, 4709 (1985).
- [23] M.V. Gorev, I.N. Flerov, V.S. Bondarev, M. Maglione, A. Simon. *FTT* **53**, 10, 1969 (2011) (in Russian).
- [24] A. Simon, J. Ravez, M. Maglione. *Solid State Sci.* **7**, 925 (2005).
- [25] Bruker AXS TOPAS V4: General profile and structure analysis software for powder diffraction data. — User's Manual. Bruker AXS, Karlsruhe, Germany. 2008.
- [26] A.V. Kartashev, I.N. Flerov, N.V. Volkov, K.A. Sablina. *FTT* **50**, 11, 2027 (2008). (in Russian).
- [27] B.A. Strukov, A.K. Ivanov-Shchits. *Kristallografiya* **18**, 4, 866 (1973). (in Russian).
- [28] D. Meyerhofer. *Phys. Rev.* **112**, 2, 413 (1958).
- [29] F. Jonah, D. Shirane. *Segnetoelektricheskie kristally*. Mir, M. (1965). 555 s. (in Russian).
- [30] S.A. Hayward, E. Salje. *Journal of Physics: Condensed Matter*. **14**, 599 (2002).
- [31] J. Gao, Y. Wang, Y. Liu, X. Hu, X. Ke, L. Zhong, Y. He, X. Ren. *Scientific Reports* **7**, 40916 (2017).
- [32] G.A. Smolenskii. *J. Phys. Soc. Jpn.* **28**, 26 (1970).
- [33] K. Uchino, Sh. Nomura. *Ferroelectrics* **44**, 55 (1982).
- [34] F. Bahri, A. Simon, H. Khemakhem, J. Ravez. *Phys. Stat. Sol. (a)* **184**, 2, 459 (2001).
- [35] G. Sebald, S. Pruvost, D. Guyomar. *Smart Mater. Struct.* **17**, 015012 (2008).
- [36] F.Y. Lee, S. Goljahi, I.M. McKinley, ChS. Lynch, L. Pilon. *Smart Mater. Struct.* **21**, 025021 (2012).
- [37] D. Sharma, S. Patel, A. Singh, R. Vaish. *J. Asian Ceram. Soc.* **4**, 102 (2016).

Translated by A.Akhtyamov